PHENIX results on flow observables in asymmetric Cu+Au collisions

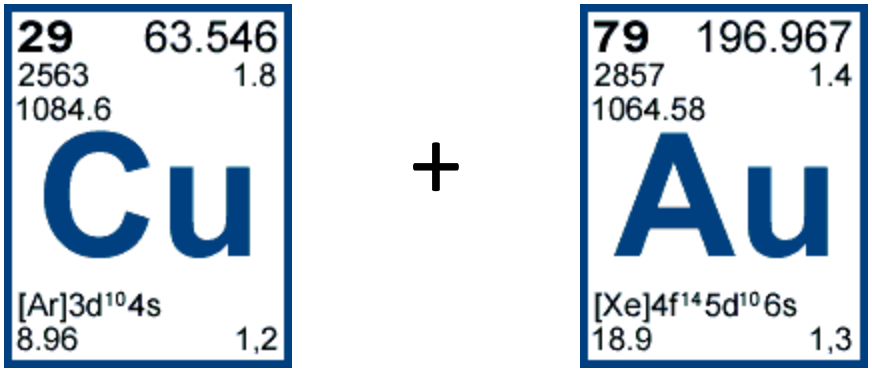

Brennan Schaefer for the PHENIX Collaboration
Vanderbilt University
28 Oct. 2015

contents

- introduction and motivation
- detector details
- directed, elliptic, and triangular flow
  - charged particle
  - identified hadron
- viscous hydro, AMPT comparison
- conclusions

Collision Systems at BNL-RHIC

- Au+Au
- p+p
- d+Au
- Cu+Cu
- U+U
- Cu+Au
- He+Au
- p+Au
- p+Al

PHENIX data in this analysis

- Run 12 (2012)
- 200 GeV
- 5 weeks
- 7.6 B events
- $|\eta| < 0.35$

anisotropic flow harmonics – event plane method

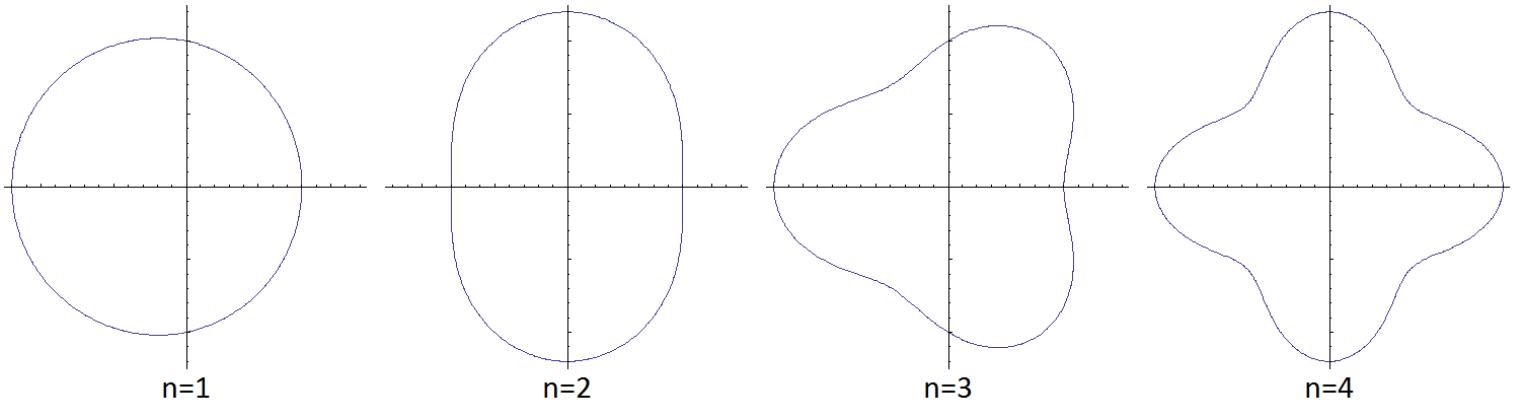

$$\frac{dN}{d\varphi} \propto \left(1 + 2\sum_{n=1}^{+\infty} v_n \cos\left[n(\phi - \psi_n)\right]\right)$$

$$v_n = \left\langle \cos\left[n\left(\phi - \psi_n\right)\right]\right\rangle$$

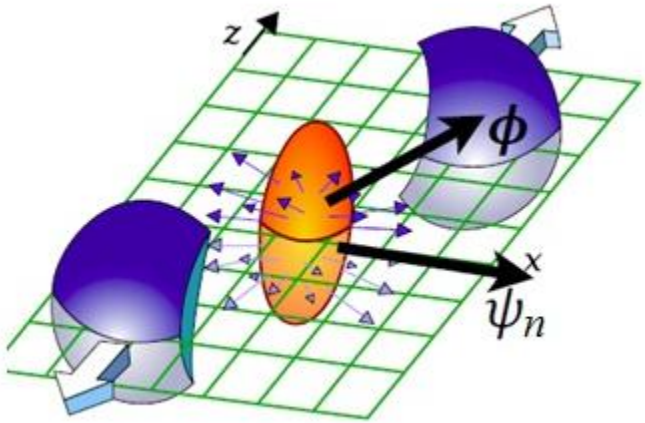

anisotropic flow harmonics – event plane method

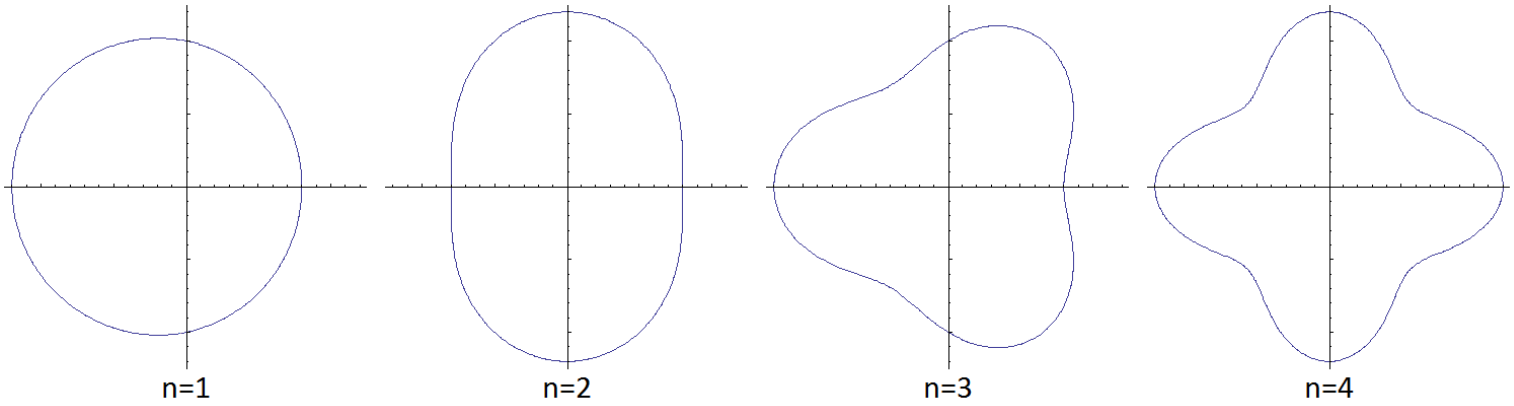

- reflect properties of initial state and evolution
- probe different length scales
- sensitive to EoS and η/s

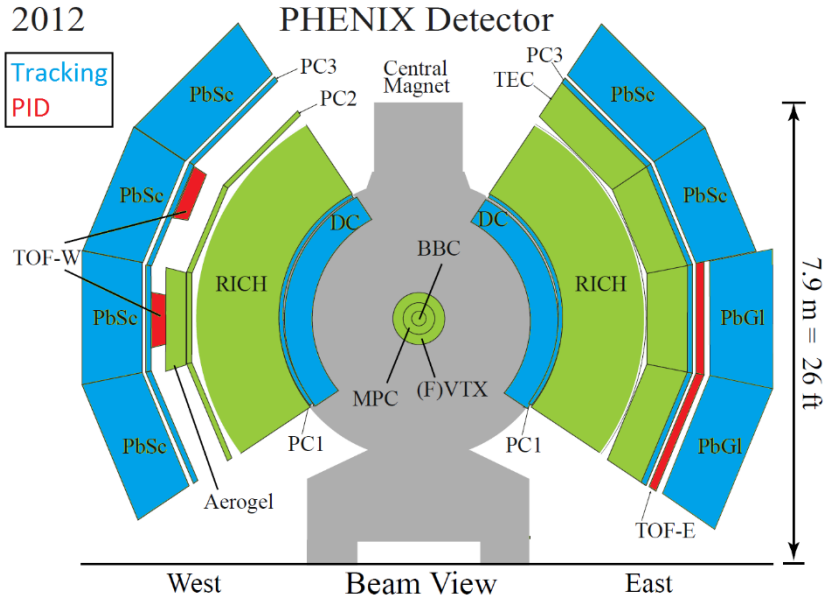

tracks reconstructed with DC and matched to PC3, EMCal

PID: TOFE, TOFW

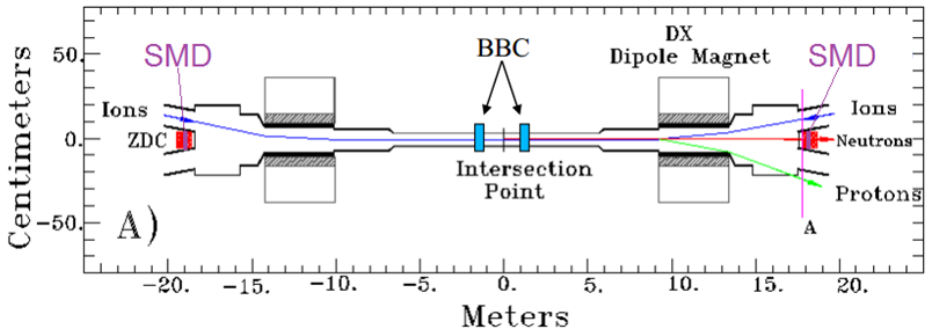

ψ_1 - *Shower Maximum Detector spectator plane*

$\psi_{2,3}$ - *Beam Beam Counter participant plane*

v_1 sign conventions used

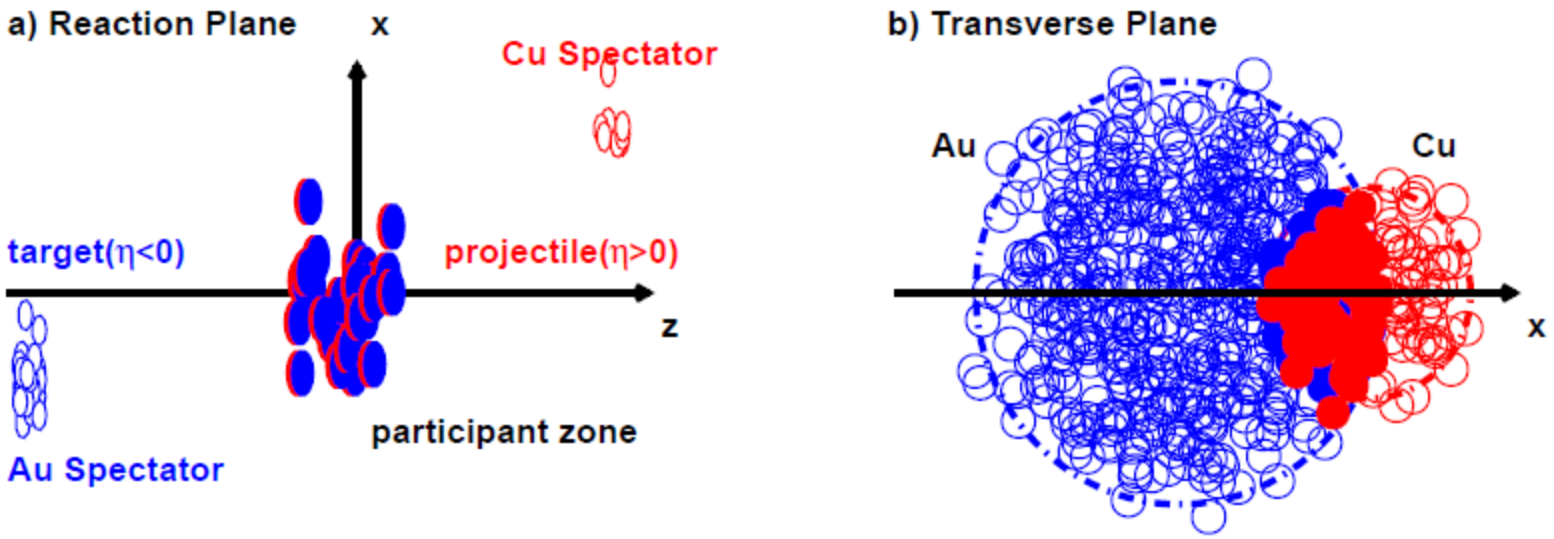

- v_1 is defined to be positive at positive η (Cu-going)
- x is positive if spectators flow outwards
- measurements use Au spectators, signs are flipped

event plane resolution

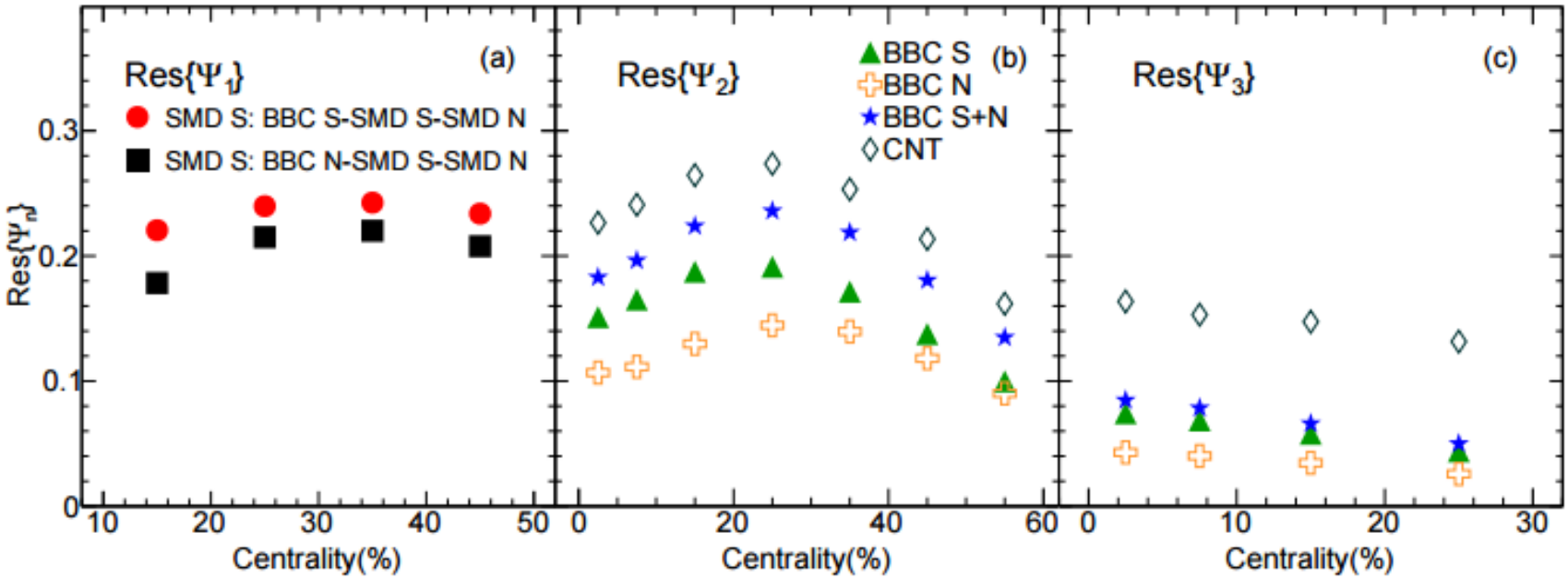

three sub-event method used to determine the resolution:

$$\mathrm{Res}(\Psi_n^A) = \sqrt{\frac{\langle \cos n\,(\Psi_n^{\mathrm{A}} - \Psi_n^{\mathrm{B}})\rangle \langle \cos n\,(\Psi_n^{\mathrm{A}} - \Psi_n^{\mathrm{C}})\rangle}{\langle \cos n\,(\Psi_n^{\mathrm{B}} - \Psi_n^{\mathrm{C}})\rangle}}$$

Ψ_1 : SMDS, $\Psi_{2,3}$: BBCS+BBSN

centrality dependence

v_1

magnitude decreases

v_2

magnitude increases

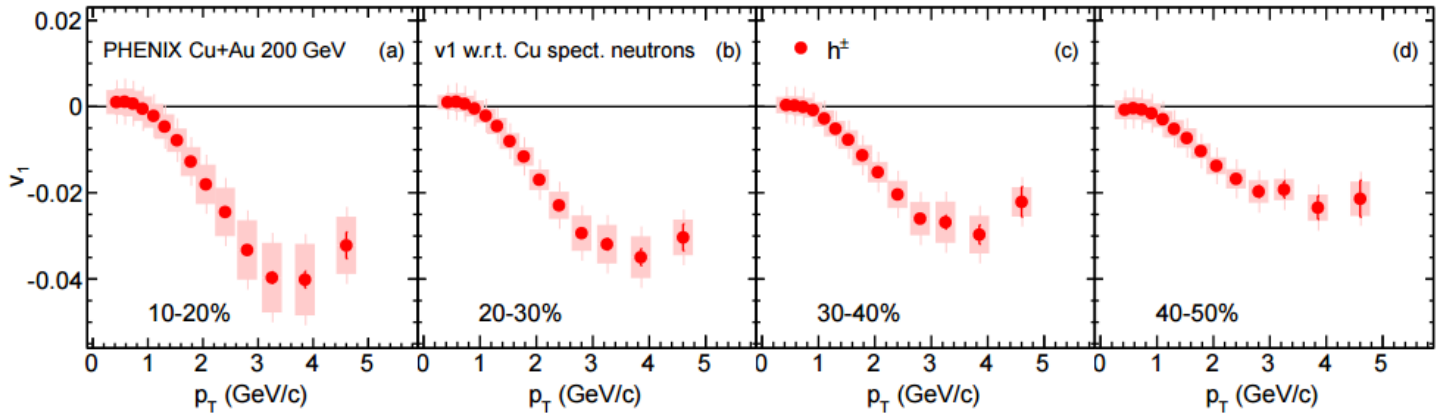

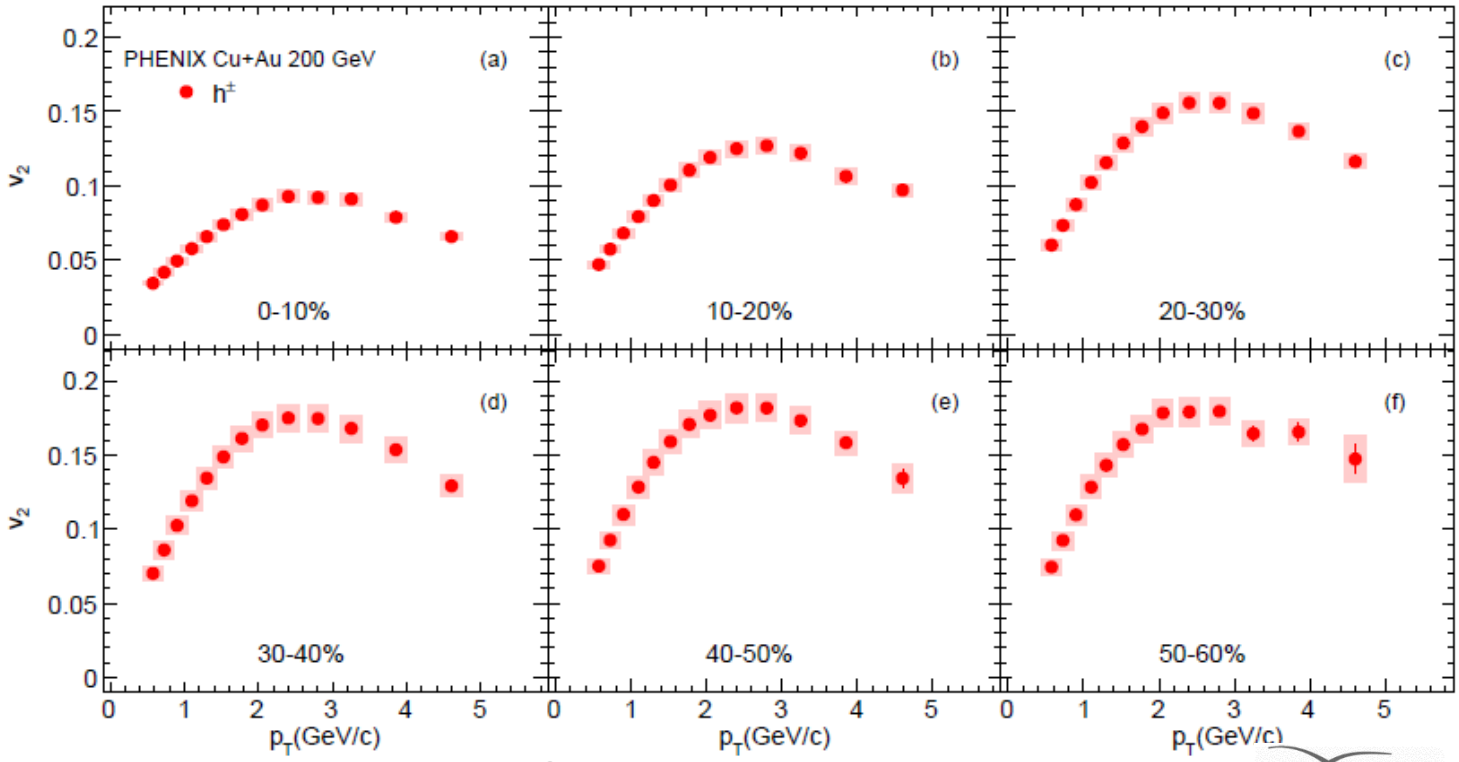

centrality dependence

v_3

weak dependence

v_2

magnitude increases

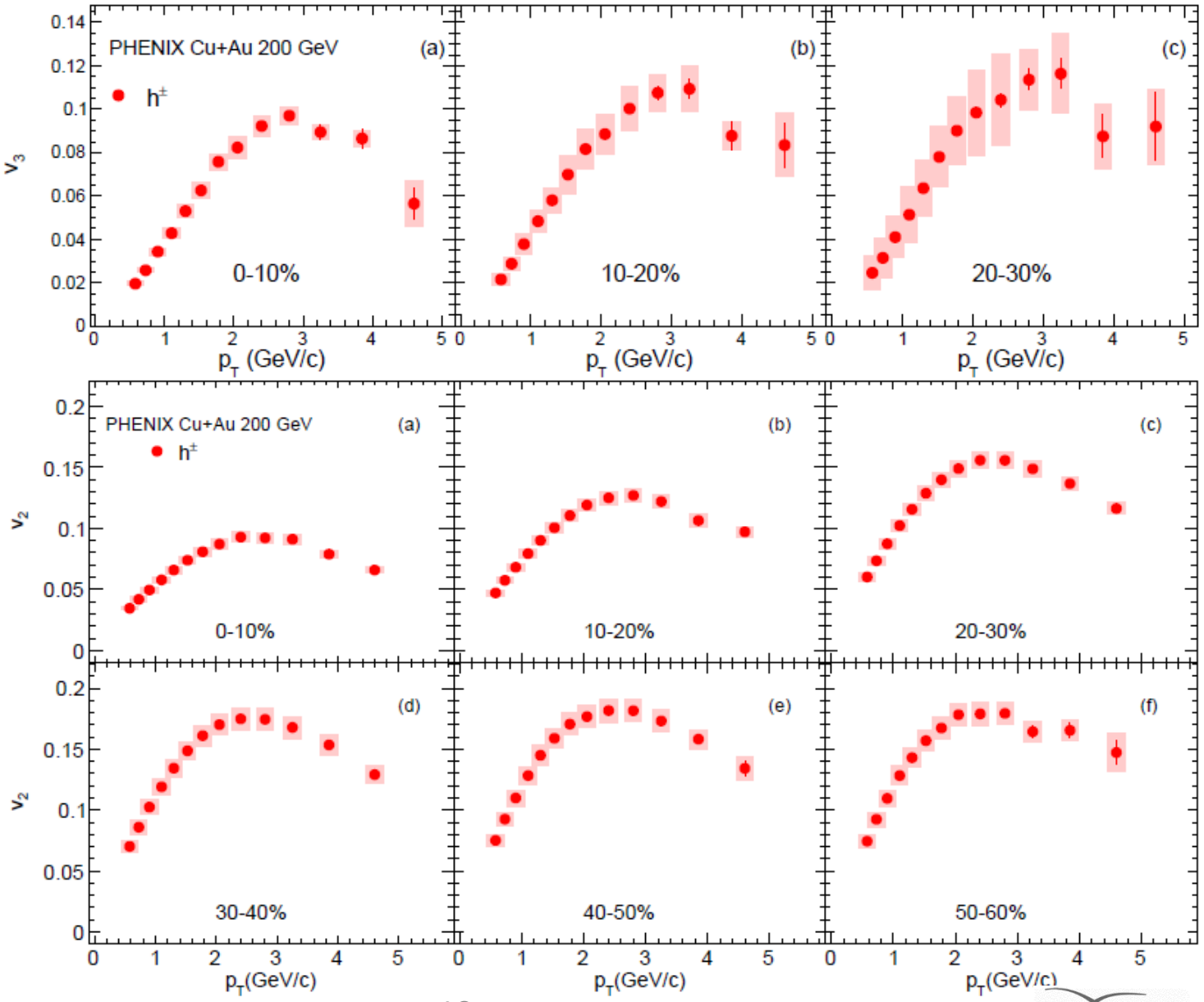

v_2 system size dependence

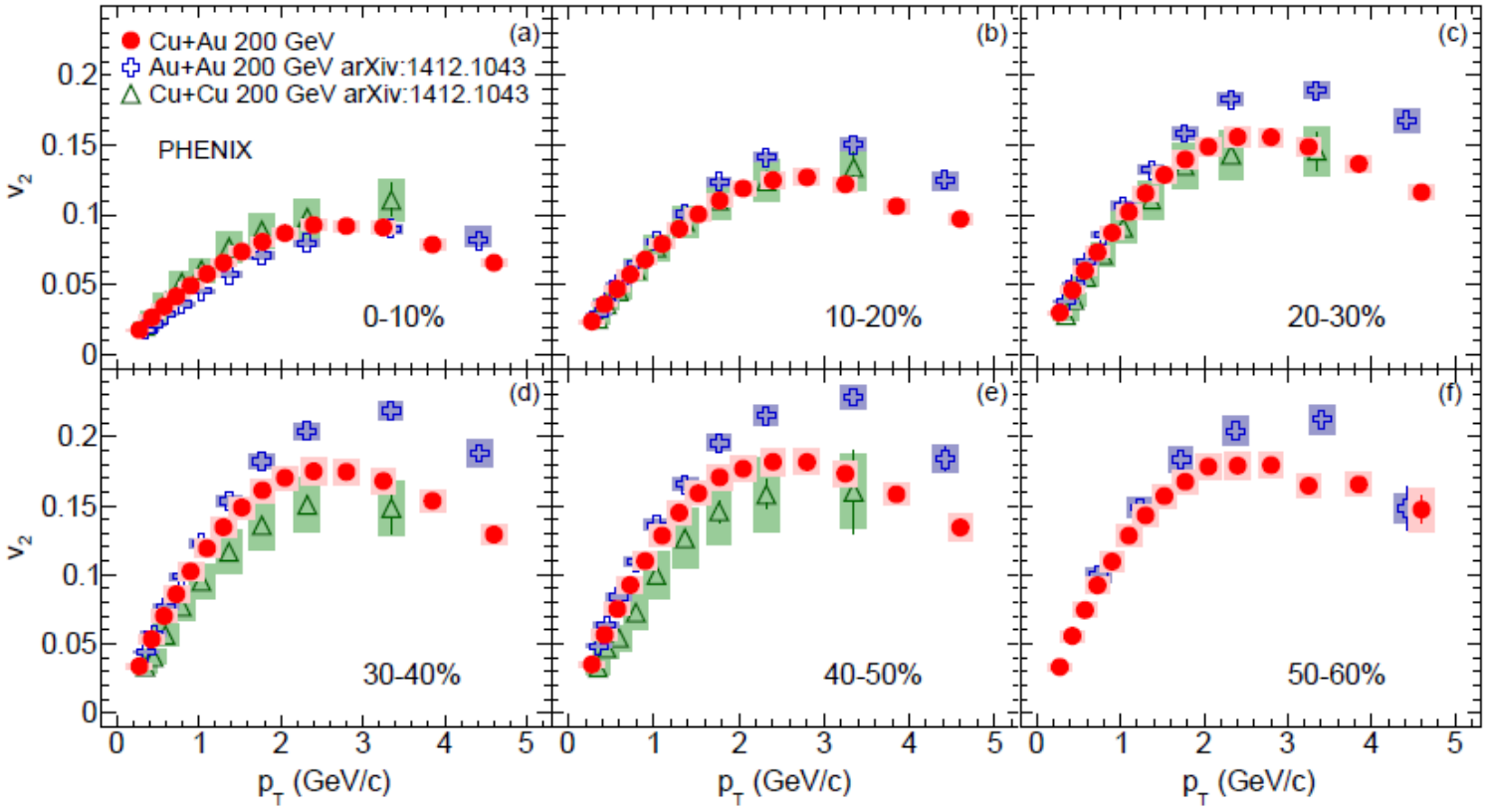

Cu+Au falls between Cu+Cu and Au+Au

v_2 (ε_2 scaled)

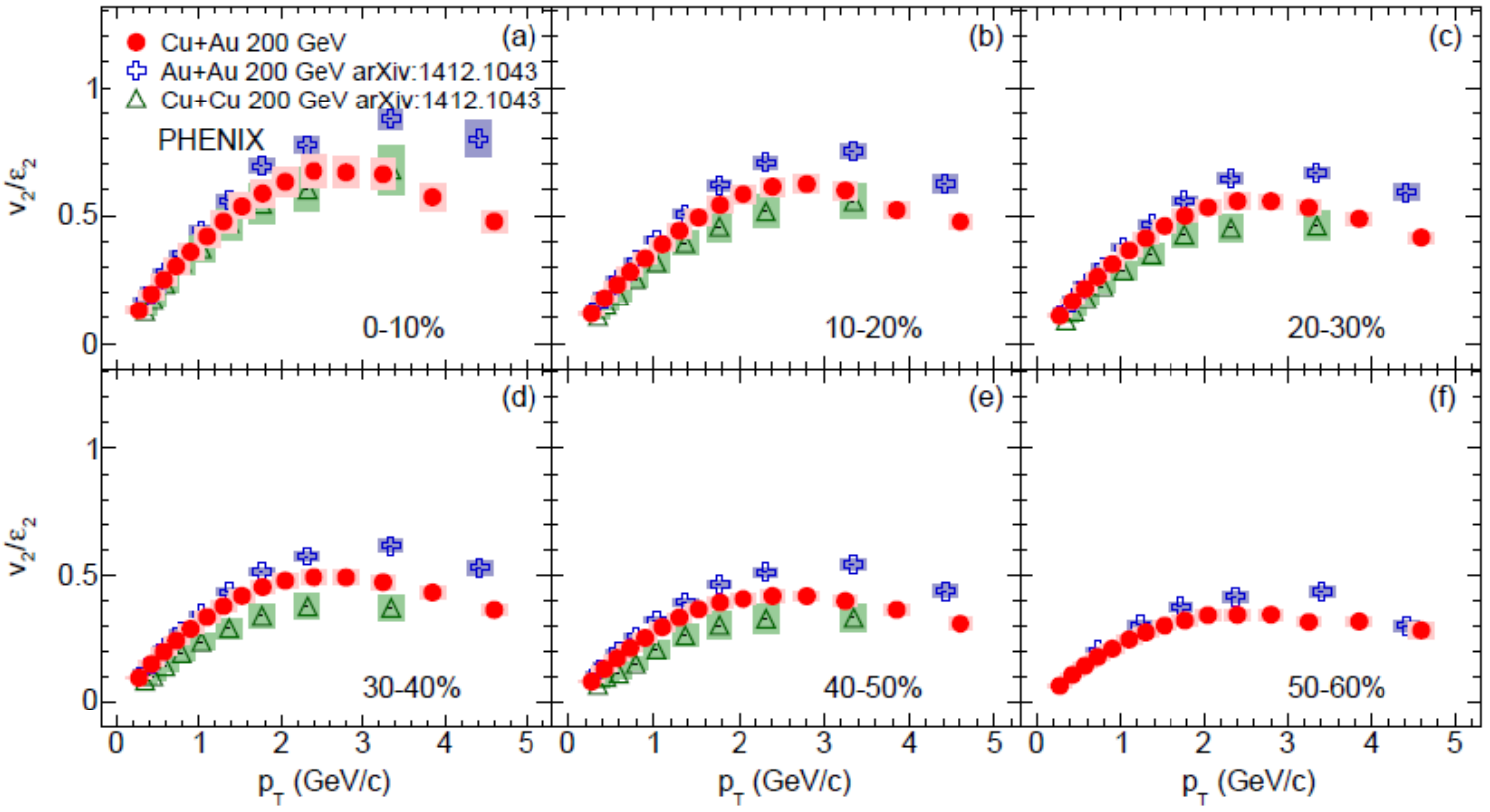

ε_2 scaling reorders the results by system size

v_2 ($\varepsilon_2 N_{part}^{1/3}$ scaled)

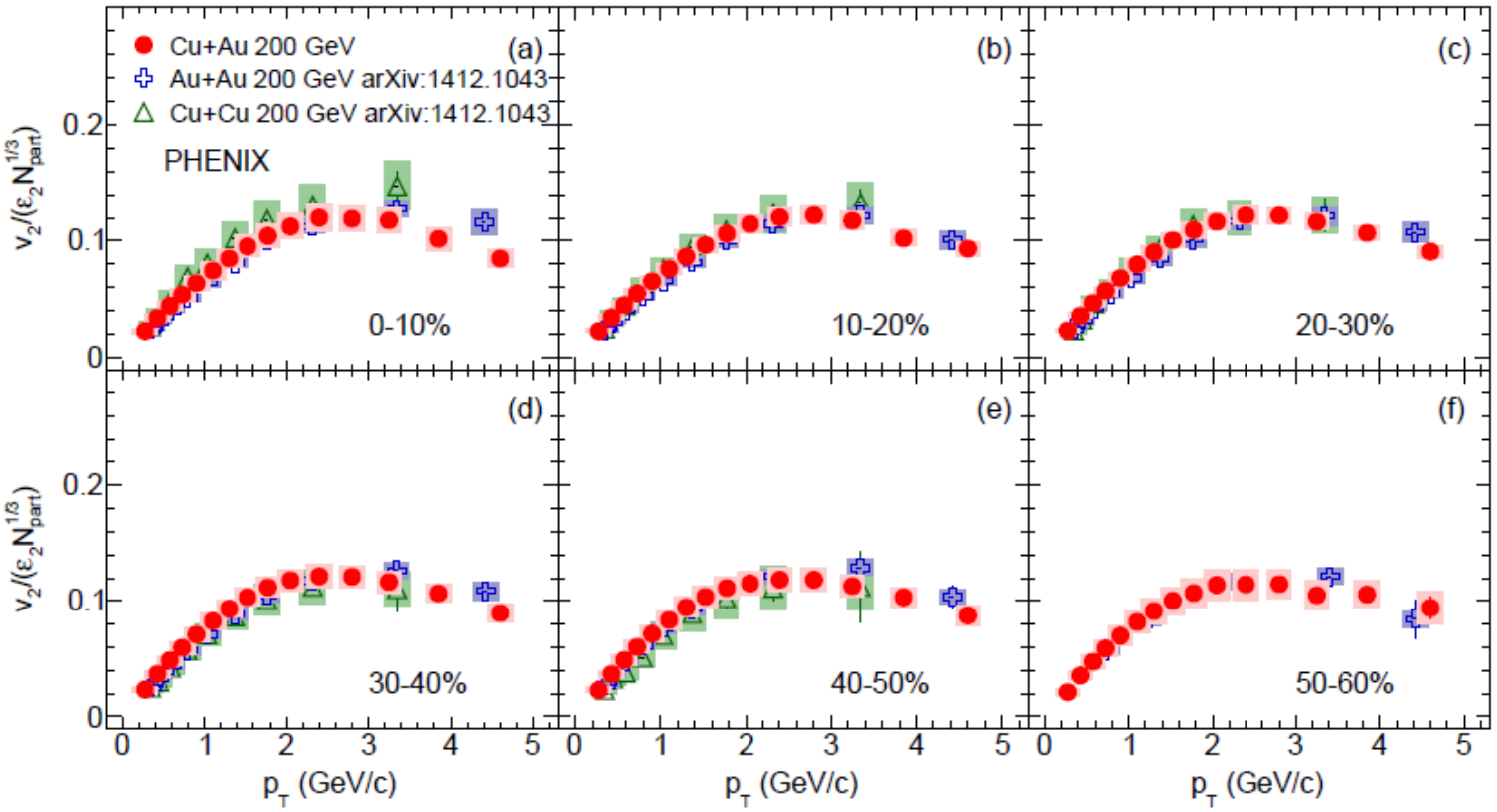

universal behavior in all centralities and systems:
Cu+Cu, Cu+Au, Au+Au

centrality bin	Au+Au 200 GeV ε_3	Cu+Au 200 GeV ε_3
0%–10%	0.087 ± 0.0018	0.130 ± 0.004
10%–20%	0.122 ± 0.0035	0.161 ± 0.005
20%–30%	0.156 ± 0.0047	0.208 ± 0.007

for the same centrality Glauber-ε_3 is larger in the smaller system due to increased fluctuations

v_3 system size dependence

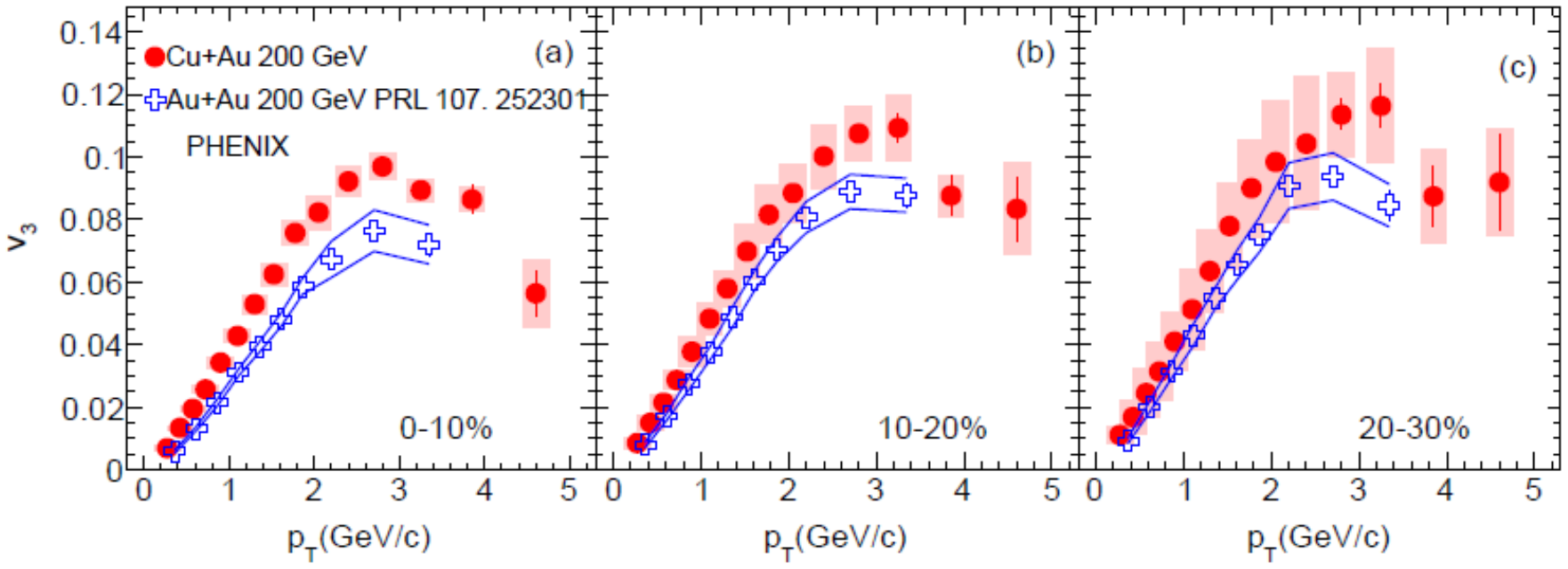

$v_{3\ \mathrm{Cu+Au}} > v_{3\ \mathrm{Au+Au}}$

v_3 (ε_3 scaled)

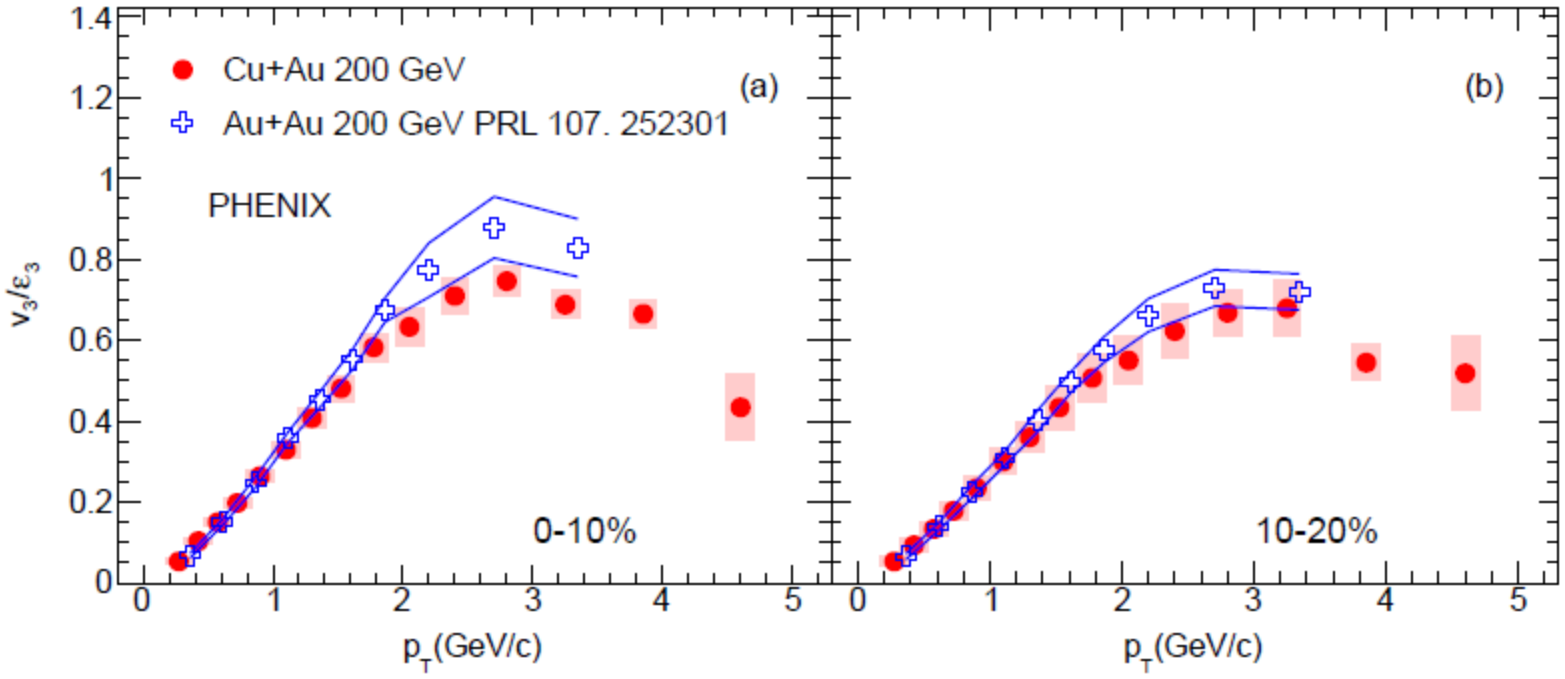

close agreement at low-intermediate p_T
within systematics at high p_T

v_3 ($\varepsilon_3 N_{part}^{1/3}$ scaled)

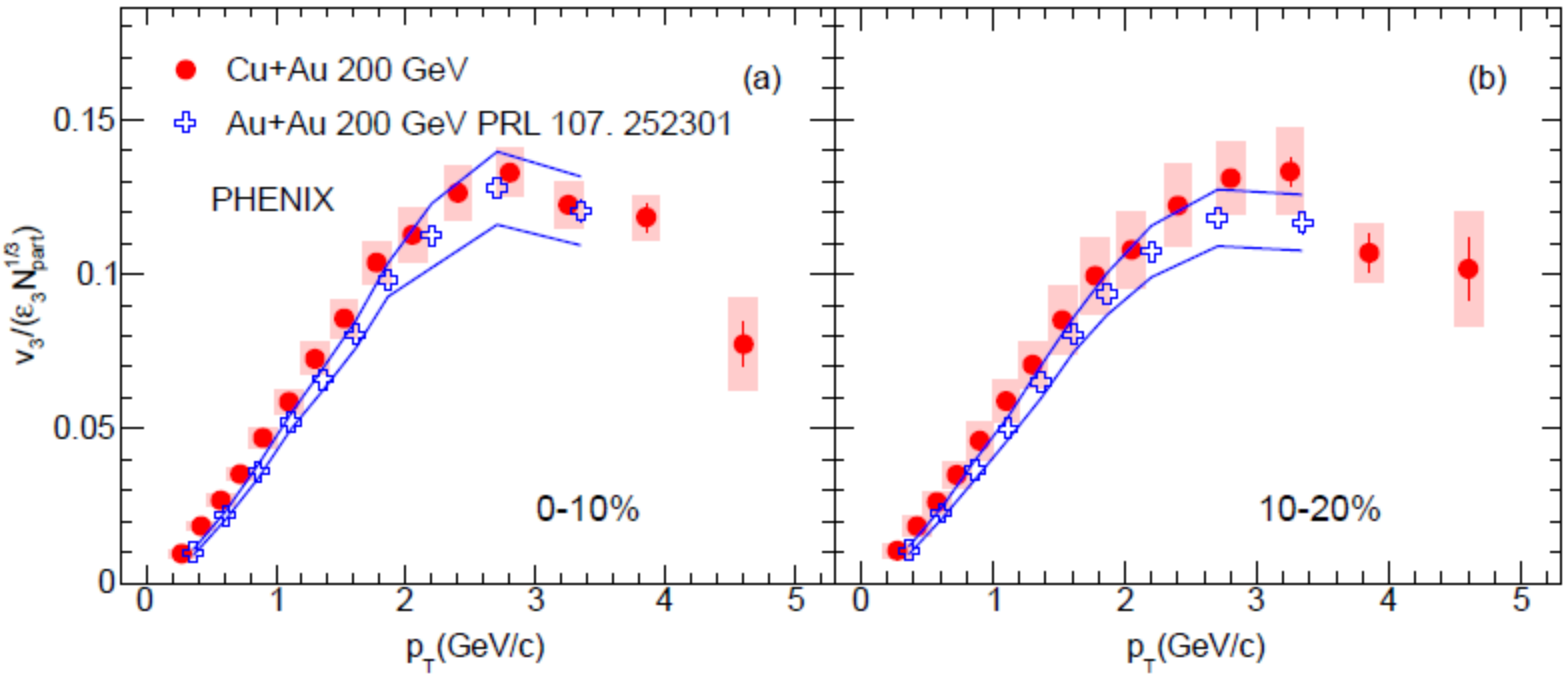

agreement within systematics at all p_T

identified particle v_2

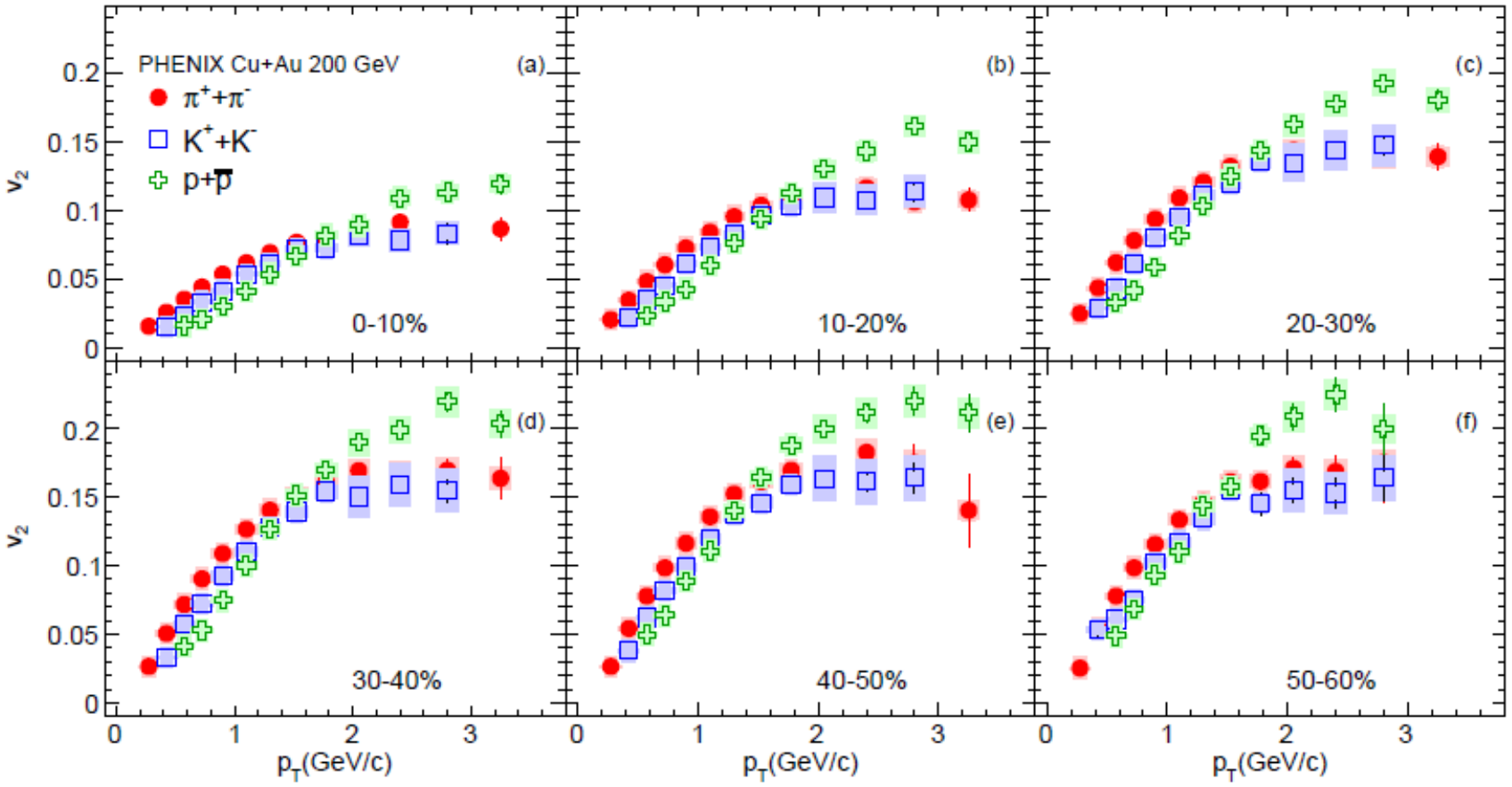

mass ordering at low p_T for v_2

identified particle $v_{1,3}$

v_1

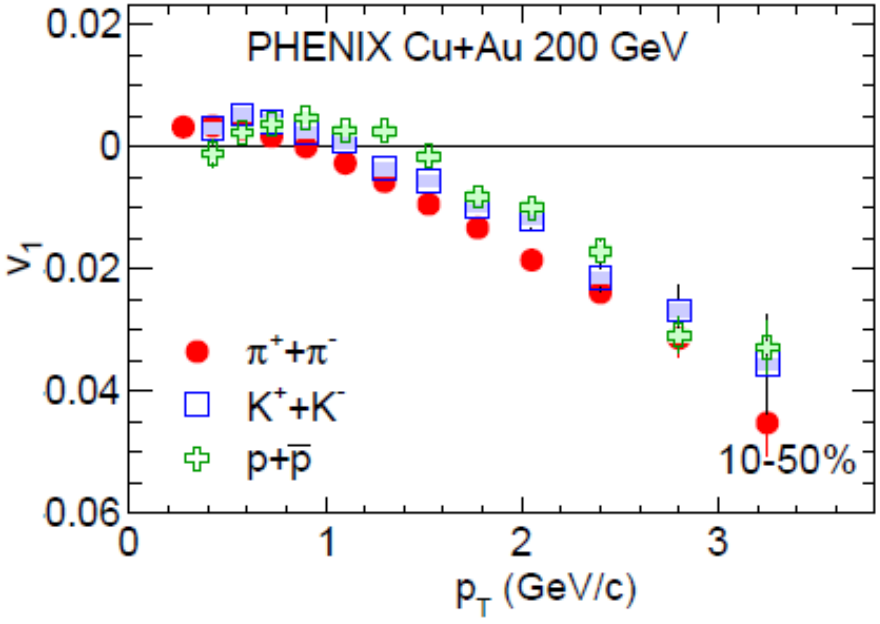

v_3

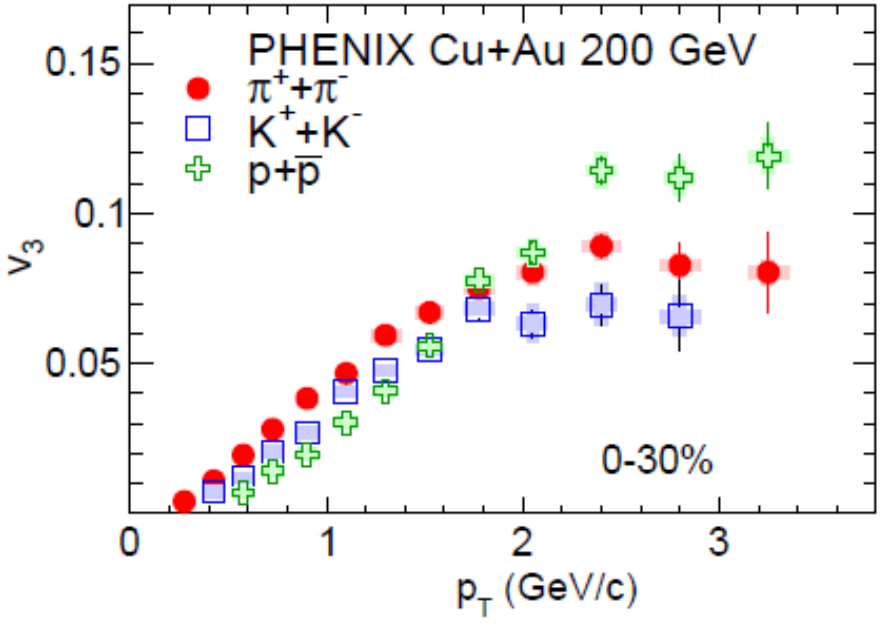

mass ordering at low p_T for $v_{1,3}$

comparison to viscous hydro

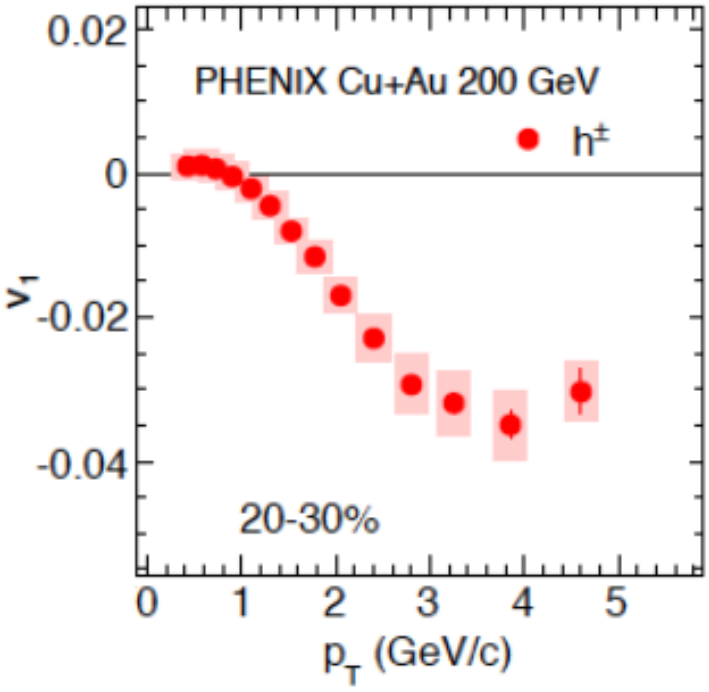

P. Bozek, Phys. Lett. B717 (2012) 287

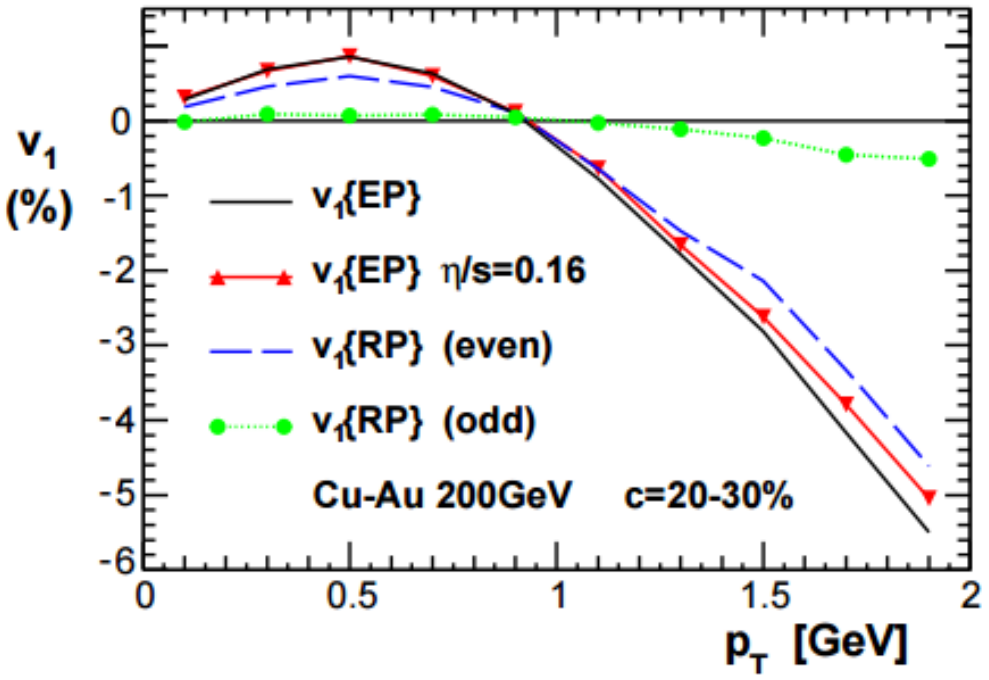

$|\eta| < 0.35$ $|\eta| < 1.0$

indirect comparison shows qualitative agreement, assuming spectators curl outward from the z-vertex

comparison to viscous hydro

v_2

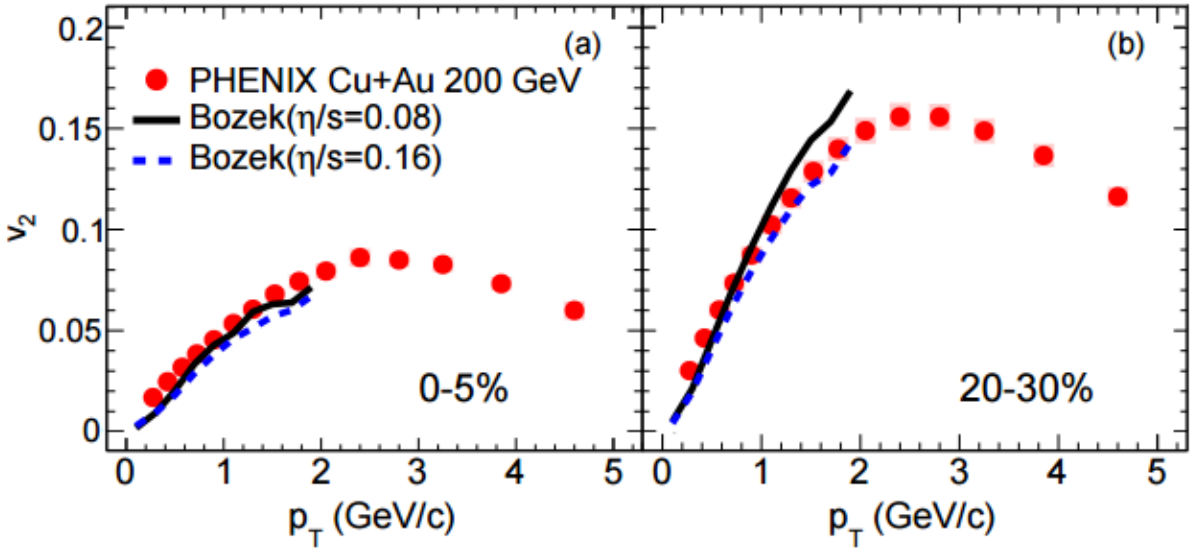

v_3

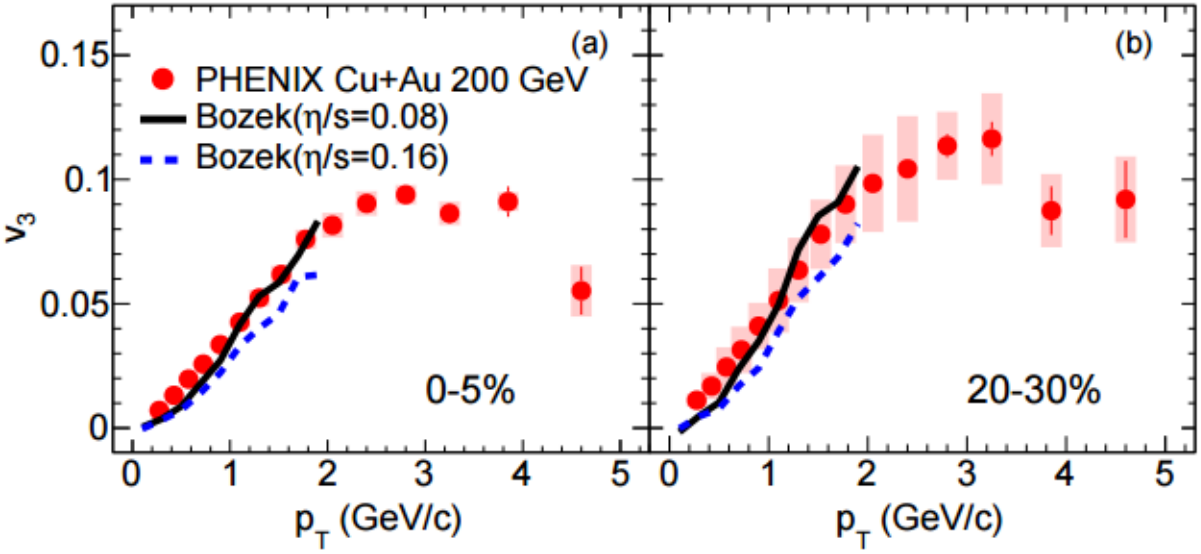

comparison to AMPT

v_2

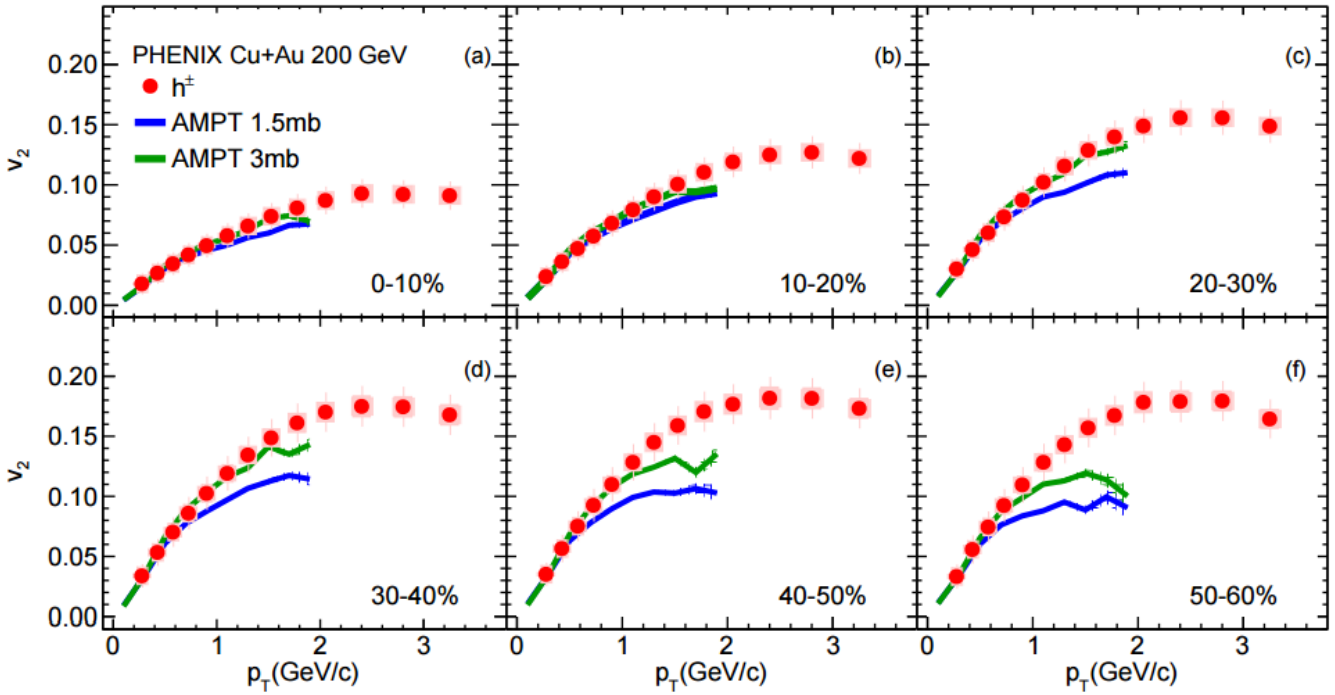

v_3

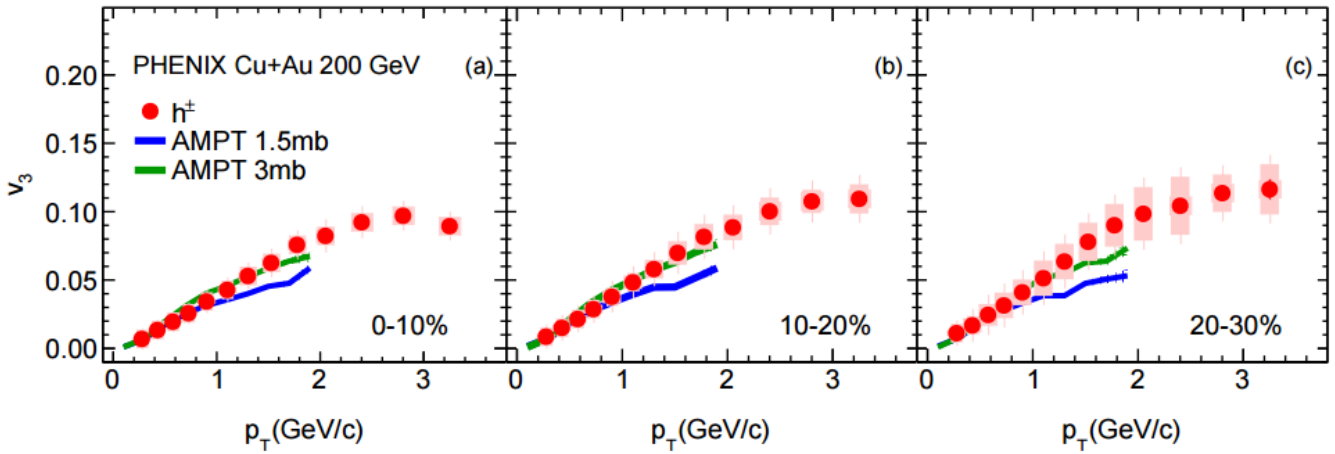

conclusions

- in Cu+Au the magnitude of v_1 decreases from central to peripheral, opposite to v_2 behavior
- $v_{2,3}$ in different systems scale with $\varepsilon_{2,3}$ $N_{part}^{1/3}$
- mass ordering is seen for all harmonics
- $v_{2,3}$ is consistent with viscous hydro $\eta/s = (1\text{-}2)/4\pi$
- AMPT with σ = 3.0 mb describes $v_{2,3}$ for $p_T < 2$ GeV

backup

Number of participant and the participant eccentricity (ε_2, ε_3) from Glauber Monte-Carlo calculations for Au+Au, Cu+Cu, and Cu+Au collisions at 200 GeV

centrality	Au+Au 200 GeV			Cu+Cu 200 GeV		Cu+Au 200 GeV		
bin	N_{part}	ε_2	ε_3	N_{part}	ε_2	N_{part}	ε_2	ε_3
0%–10%	325.2	0.103	0.087	98.2	0.163	177.2	0.138	0.130
	±3.3	±0.003	± 0.0018	±2.4	±0.003	±5.2	±0.011	±0.004
10%–20%	234.6	0.200	0.122	73.6	0.241	132.4	0.204	0.161
	±4.7	±0.005	± 0.0035	±2.5	±0.007	±3.7	±0.008	±0.005
20%–30%	166.6	0.284	0.156	53.0	0.317	95.1	0.280	0.208
	±5.4	±0.006	± 0.0047	±1.9	±0.006	±3.2	±0.008	±0.007
30%–40%	114.2	0.356	0.198	37.3	0.401	65.7	0.357	0.266
	±4.4	±0.006	± 0.0083	±1.6	±0.008	±3.4	±0.010	±0.010
40%–50%	74.4	0.422	0.253	25.4	0.484	43.3	0.436	0.332
	±3.8	±0.006	± 0.0111	±1.3	±0.008	±3.0	±0.013	±0.013
50%–60%	45.5	0.491	0.325	16.7	0.579	26.8	0.523	0.412
	±3.3	±0.005	± 0.0179	±0.9	±0.008	±2.6	±0.019	±0.019

backup

Systematic uncertainties given in percent on the v_n measurements.

v_n	Uncertainty Sources	10%–20%	40%–50%	Type
v_1	Event plane resolution	20%	12%	C
	Event plane detectors	3%	4%	B
	Background	2%	2%	A
	Acceptance	10%	10%	C
v_2	Event plane resolution	2%	2%	C
	Event plane detectors	3%	4%	B
	Background	2%	2%	A
	Acceptance	8%	3%	C
v_3	Event plane resolution	2%	2%	C
	Event plane detectors	3%	7%	B
	Background	2%	2%	A
	Acceptance	2%	10%	C

backup

Systematic uncertainties for particle identification

species	$p_T \leq 2\text{GeV}/c$	$p_T \geq 2\text{GeV}/c$	Type
pion	3%	5%	A
kaon	3%	10%	A
proton	3%	5%	A